ENVIRONMENTAL SCIENCE

Miocene flooding events of western Amazonia

Carlos Jaramillo,[1]* Ingrid Romero,[1,2,3] Carlos D'Apolito,[1,3,4] German Bayona,[3] Edward Duarte,[3] Stephen Louwye,[5] Jaime Escobar,[6] Javier Luque,[7] Jorge D. Carrillo-Briceño,[8] Vladimir Zapata,[9] Alejandro Mora,[10] Stefan Schouten,[11] Michael Zavada,[12] Guy Harrington,[4] John Ortiz,[1] Frank P. Wesselingh[13]

There is a considerable controversy about whether western Amazonia was ever covered by marine waters during the Miocene [23 to 5 Ma (million years ago)]. We investigated the possible occurrence of Miocene marine incursions in the Llanos and Amazonas/Solimões basins, using sedimentological and palynological data from two sediment cores taken in eastern Colombia and northwestern Brazil together with seismic information. We observed two distinct marine intervals in the Llanos Basin, an early Miocene that lasted ~0.9 My (million years) (18.1 to 17.2 Ma) and a middle Miocene that lasted ~3.7 My (16.1 to 12.4 Ma). These two marine intervals are also seen in Amazonas/Solimões Basin (northwestern Amazonia) but were much shorter in duration, ~0.2 My (18.0 to 17.8 Ma) and ~0.4 My (14.1 to 13.7 Ma), respectively. Our results indicate that shallow marine waters covered the region at least twice during the Miocene, but the events were short-lived, rather than a continuous full-marine occupancy of Amazonian landscape over millions of years.

INTRODUCTION

The Neogene history of Amazonia is essential for understanding the evolution of the rainforest and associated fauna living in one of the most diverse places on Earth (1). A central question about our understanding of Amazonia remains unsolved: Did continental-scale marine flooding occur in western Amazonia during the Neogene? Miocene marine transgressions in the continental interior would have had a profound effect on the diversification and structuring of both terrestrial and aquatic Neotropical communities (1–6).

To date, about 80% of Amazonian landscape is occupied by terra-firme forest, where flooding is rare, whereas ~20% is characterized by wetlands (annually flooded floodplains with isolated lakes and river-bound oxbows) (7, 8). Flooded and terra-firme forests have distinctive floras that are among the most diverse on the planet (9). However, during the Miocene, the situation in western Amazonia was very different. Widespread occurrence of Miocene sediments indicates that subsidence of western Amazonian basins was active, extensive (1, 10), and probably driven by plate-mantle interaction associated with the rise of the Andes (11). These Miocene sediments, known as the Solimões, Pebas, and Acre formations, are on average 250 to 300 m thick but, in some places, can be more than 1000 m in thickness (12, 13). Many of these sediments have been studied over the years (for a more comprehensive list of publications, see the Supplementary Materials) (14–19). Previous investigations focused primarily on isolated river outcrops, where generally only 5 to 60 m of strata are exposed. Lack of exposure makes it very difficult to study a complete and continuous Miocene sequence.

There are several conflicting interpretations of the Miocene depositional environment in western Amazonia. They include (i) an epi-continental shallow sea that covered the Amazon for millions of years (4, 20); (ii) a large freshwater megalake, either long-lived Neogene [15 My (million years)] or Pleistocene-Holocene (16); (iii) a fluvio-lacustrine system with extensive floodplains and a few marine incursions (17, 21–23); (iv) a high frequency of transgressive-regressive bay-margin successions (18, 24); (v) avulsive fluvial belts in a floodbasin-floodplain environment lacking marine influence (12, 25); (vi) a long-lived [23 to 8 Ma (million years ago)] megalake/wetland system (or "para-marine megalake," as it is an environment without a modern analog), composed of widespread and semipermanent aquatic ecosystems (26, 27); (vii) a complex series of interconnected megalakes overlying a regional pene-plain (14); and (viii) a tidal system (28). All of these interpretations involve discussion of the evidence for marine incursions during the Neogene. Did they occur, and if so, how frequently and for how long?

All recent studies show a biogeographic connection between western Amazonia and the Llanos Basin of Colombia during most of the Miocene (4, 20, 22, 26, 29), yet direct evidence for a marine pathway is lacking. Marine incursion into Amazonia, if any, should have come primarily throughout the Colombian Llanos (3, 18, 20) and the Venezuelan Barinas/Apure and Eastern basins (fig. S1) (19). We analyzed age, fossil record, geochemistry, and depositional environments on two cores from a nearly horizontal Miocene sequence in the Llanos and Amazonas/Solimões basins, together with seismic information and electric logs, to identify the timing, duration, and frequency of marine floodings during the Miocene in western Amazonia (see Fig. 1, fig. S2, Materials and Methods, and the Supplementary Materials).

RESULTS

Marine intervals

A total of 933 palynomorph types and 54,141 individuals were counted and identified from the cores Saltarin and 105-AM (tables S1 and S2). Saltarin has two stratigraphic intervals composed of laminated, greenish mudstones that contain a high proportion of marine palynomorphs (MPs) (see Fig. 1, figs. S3 and S4, and the Supplementary Materials). The lower interval spans 645.6 to 617.6 m (MP mean = 24.3%; table S3), and the second interval spans 548 to 408.4 m (MP mean = 39.6%; table S3). The high MP percentages in those intervals contrast with a significantly lower proportion of MPs in interbedded intervals (interval
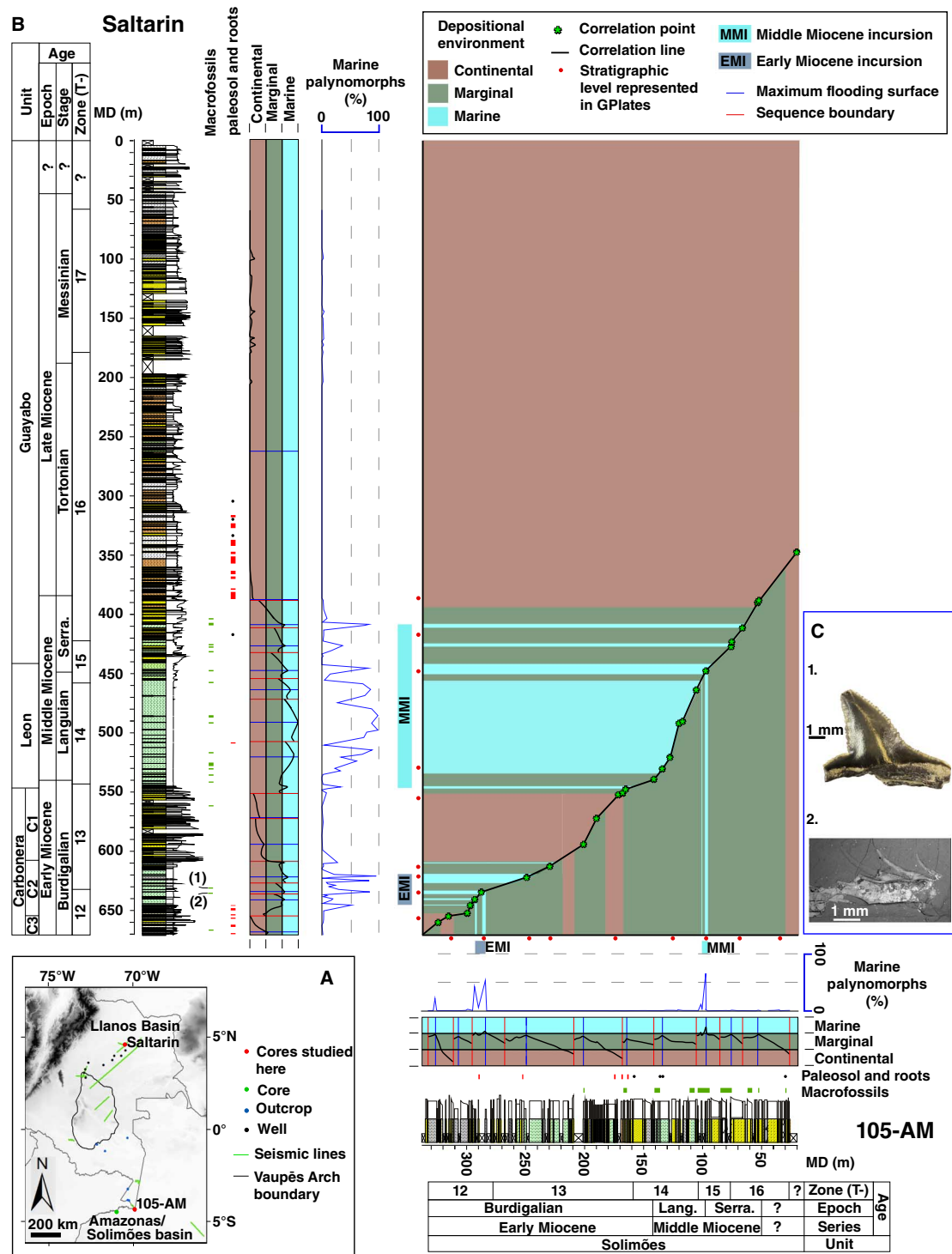
Fig. 1. Core correlation and marine intervals in the Llanos and Amazonas/Solimões basins. (**A**) Location of seismic lines, wells, and outcrops used in this study in the Llanos Basin of Colombia and in the Amazonas/Solimões Basin near the Colombia-Brazil boundary. (**B**) Correlation of the stratigraphic units drilled in the Saltarin and 105-AM wells using age control established by palynology and sequence stratigraphy analysis. The depositional environment interpretation and the abundance of MPs identify the two intervals of marine incursions, the early Miocene incursion (EMI) and the middle Miocene incursion (MMI), in each well and indicate thicker deposition of marine deposits in the Llanos Basin. Biostratigraphic zones (T-) follow those in the study of Jaramillo *et al.* (*56*). MD, meters depth. (**C**) Macrofossils found in the Saltarin well: (1) tooth of a Carcharhiniformes shark (fig. S6) and (2) mantis shrimp (fig. S7). These fossils are further evidence of the marine incursion that covered the Llanos Basin. See the Supplementary Materials for a detailed description and identification of these fossils. Depositional environments were grouped into three broad categories: (i) Continental environment that represents accumulation in fluvial channels and adjacent floodplains by subaerial exposure; (ii) Marginal environment that represents accumulation on deltaic plains; low-energy wetlands with swamps, ponds, and channels; and shallow freshwater lacustrine systems; and (iii) Marine environment that represents shallow marine water. Notice that the Marine environment of 105-AM is shallower and less saline than the marine intervals in Saltarin.

>645.6 m, MP mean = 2.7%; interval 617.59 to 548.1 m, MP mean = 3.9%; interval <408.4 m, MP mean = 0.9%; $P < 0.01$, t test; df = 53.2; Supplementary Materials), which are dominated by fine- to coarse-grained sandstones of the Continental environment (see Fig. 1, figs. S3 and S4, and the Supplementary Materials). The MP assemblage comprises 8 species of dinoflagellates/acritarchs in the lower interval and 25 species in the upper interval (see fig. S5, table S1, and the Supplementary Materials). The relatively low values of the branched versus isoprenoidal tetraether (BIT) index for both the lower interval (BIT mean = 0.26; SD = 0.14; $n = 5$) and upper interval (BIT mean = 0.3, SD = 0.2, $n = 13$) also indicate high input of marine-dwelling Thaumarchaeota and low input of soil-derived tetraether lipids that are typical for shallow marine sections (table S4) (30) and are significantly lower than BIT values for the modern Amazon Basin ($P < 0.001$, t test; df = 34.12) [modern values are reported in Table 3 of Zell et al. (31)]. Two macrofossils in the lower marine stratigraphic interval also indicate a marine environment. The first is a shark tooth at 630.08 m, identified as Carcharhiniformes gen. et sp. indet. (Carcharhinus or Sphyrna) (see Fig. 1, fig. S6, and the Supplementary Materials). Representatives of this shark group are common inhabitants of marine environments, although some species can tolerate low salinity levels (brackish environments) (32). A second macrofossil, recovered at 636 m, was identified as Squillidae (see Fig. 1, fig. S7, and the Supplementary Materials). Squillids are strictly marine stomatopods that dwell in burrows in soft, muddy to sandy sediments of tropical and subtropical low intertidal to shallow subtidal habitats (33). The proportion of lacustrine palynomorphs is low across the section (mean = 3.4%) and varies little among the five stratigraphic intervals (table S3).

The core 105-AM also has two stratigraphic intervals with a high proportion of MPs, but the intervals are much thinner than those at Saltarin (Fig. 1 and figs. S4 and S8). The lower interval spans 293.3 to 284 m (MP mean = 33.8%; table S3), and it is composed of claystones, with organic matter and palynomorphs of the Marine environment grading to sublitharenites of the Marginal environment (fig. S8). The second interval, spanning 101.4 to 96.7 m (MP mean = 16.3%), consists of mollusk-rich carbonaceous siltstones with palynomorphs of the marine environment (fig. S8). The mean proportion of MPs in these intervals is significantly higher than in the interbedded intervals (interval >293.3 m, MP = 2.4%; interval 283.9 to 101.5 m, MP = 0.1%; interval <96.7 m, MP = 0.1%; $P < 0.04$, t test; df = 7) (see the Supplementary Materials). Intermarine intervals are dominated mostly by the Marginal environment and composed of sandstones, lignites, and paleosols in the muddy facies. Cross-bedded sandstones are registered in strata underlying the lower marine interval, whereas strata overlying the upper marine interval show a significant increase in sandstone interbeds and a decrease in macrofossils (Fig. 1 and fig. S8). The MP assemblage comprises 15 species of dinoflagellates and acritarchs in the lower interval and 10 species in the upper interval (fig. S5 and table S2). The proportion of lacustrine palynomorphs is low across the section (mean = 3.9%) and similar among the five stratigraphic intervals (table S3). The variation of lithological associations in both marine intervals of 105-AM, the short periods of subaerial exposure to develop paleosols in the lower marine interval, and the lower proportion of MPs in both intervals compared to those in Saltarin indicate that the Marine environment of 105-AM is shallower and less saline than the marine intervals in Saltarin (Fig. 1 and table S3).

Both marine intervals in Saltarin produce two well-defined subtabular, parallel seismic intervals that can be traced throughout the entire Llanos Basin, indicating their widespread extension. These two intervals were deformed near the Vaupés Arch during the late Miocene (34). Although this arch separates the Llanos Basin from the Amazonas/Solimões Basin, seismic data suggest that during the early and middle Miocene, the arch was not active and both marine incursions extended farther to the south, reaching the Amazonas/Solimões Basin (see Fig. 2, figs. S9 and S10, and the Supplementary Materials).

The biostratigraphic and sequence stratigraphic analyses of Saltarin (see the Supplementary Materials) indicate that the core spans the early to the late Miocene, biostratigraphic zone T-12 Horniella lunarensis to zone T-17 Cyatheacidites annulatus, 18.5 to 5.5 Ma (see Fig. 1, fig. S11, and the Supplementary Materials). The lower marine interval (645.6 to 617.6 m) extends from zones T-12 to T-13, ~18.1 to 17.2 Ma, respectively, early Miocene, lasting ~0.9 My (Figs. 1 and 2 and fig. S4). The upper marine interval (548 to 408.4 m) extends from zones T13 to T16, 16.1 to 12.4 Ma, respectively, middle Miocene, spanning ~3.7 My (Fig. 1 and fig. S4).

Graphic correlation of 105-AM indicates that the core spans the early to the late Miocene, biostratigraphic zone T-12 Horniella lunarensis to zone T-16 Fenestrites spinosus, 18.8 to 10.7 Ma (see Fig. 1, fig. S12, and the Supplementary Materials). The lower marine interval (293.3 to 284 m) lies within zone T-12, 18.0 to 17.8 Ma, early Miocene, lasting ~0.2 My (Figs. 1 and 2). The upper marine interval (101.4 to 96.7 m) lies within zone T-15, 14.1 to 13.7 Ma, middle Miocene, lasting ~0.4 My (Figs. 1 and 2 and fig. S4).

DISCUSSION

Hoorn et al. (1) described three major phases in Amazonia: (i) 24 to 16 Ma, lacustrine conditions alternating with episodes of fluvial drainage and marginal marine influence; (ii) 16 to 10.5 Ma, maximum extent of lacustrine conditions with a marginal marine influence; and (iii) 10.5 to ca. 7 Ma, complex environment of deltaic, estuarine, and fluvial environments. Our results indicate that both the Llanos and Amazonas/Solimões basins of western Amazonia experienced two distinct marine transgressions (Figs. 1 and 2 and fig. S4). In the Llanos Basin, the first marine transgression completely covered the basin during the early Miocene and lasted ~0.9 My (18.1 to 17.2 Ma). This transgression event is also registered in the Amazonas/Solimões Basin in northwestern Amazonia, but its duration was much shorter there, lasting only ~0.2 My (18.0 to 17.8 Ma) (Figs. 1 and 2 and fig. S4). The second transgression in the Llanos Basin occurred during the middle Miocene and lasted ~3.7 My (16.1 to 12.4 Ma). This transgression event continued toward the Amazonas/Solimões Basin in northwestern Amazonia, but there, it lasted a much shorter time, only ~0.4 My (14.1 to 13.7 Ma) (Figs. 1 and 2 and fig. S4). All evidence indicates that marine incursions transformed fluvio-lacustrine landscapes into a gently sloping marine environment, being shallower and with lower salinities in 105-AM than in Saltarin. In both marine intervals, the onset of the transgression occurred earlier in the Llanos Basin or at the same time in the Amazonas/Solimões Basin and lasted longer in the former (Figs. 1 and 2 and fig. S4). This geographic pattern would be expected if transgression progressed from the Caribbean into western Amazonia, as many have suggested (3, 18–20). Our data suggest that the Llanos Basin transformed into a fluvial basin around 11.5 Ma, as Saltarin indicates, a condition that still prevails today (Figs. 1 and 2, figs. S3 and S4, and the Supplementary Materials) (34). Therefore, any possible late Miocene incursion into western Amazonia (3) would have been derived from pathways other than the Llanos, like the Amazon trunk valley. Correlation of these two events with strata in Putumayo, Napo, Pastaza/Marañon, Acre, Ucayali, and Madre de Dios basins (fig. S1) remains uncertain and is beyond the scope of the present analysis.
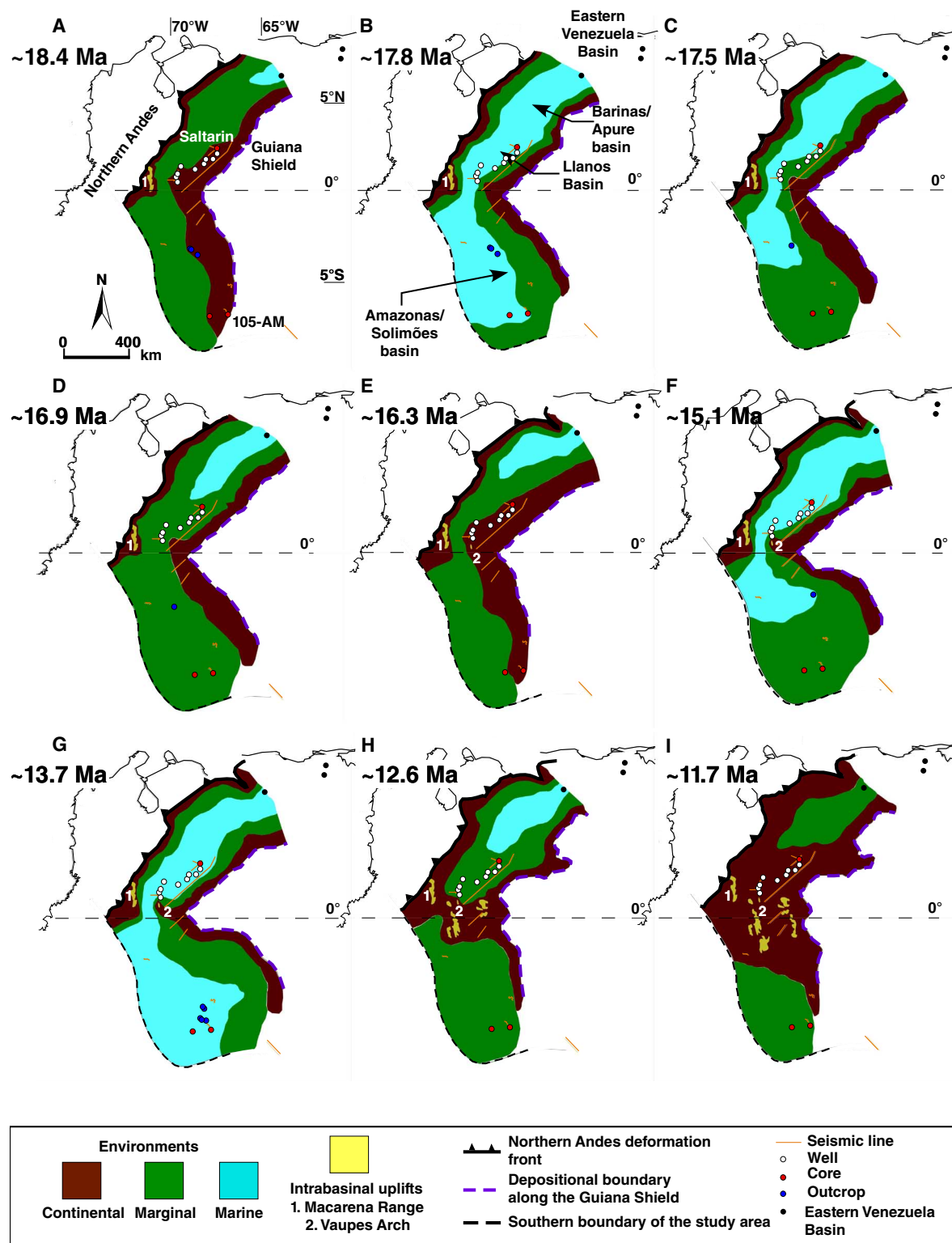
Fig. 2. Paleogeographic reconstruction of the two marine incursions in the study. (**A** to **I**) The reconstruction is based on the stratigraphic correlation shown in Fig. 1 and on the stratigraphic analysis of nine wells in the Llanos Basin and one well and nine outcrops in the Amazonas/Solimões Basin (see the Supplementary Materials for descriptions of sections and a movie based on the construction of 30 paleogeographic maps). Marine ingressions occurred earlier in the Llanos Basin than in the Solimões Basin. The two basins were separated during the late Miocene (G, H, and I) by the uplift of the Vaupés Arch. Notice that marine intervals are shallower and less saline toward the 105-AM region.

The thin nature of both marine intervals in 105-AM (9.3 and 4.5 m) could explain the large discrepancy in interpretations about possible marine incursions in Amazonia (see the Supplementary Materials for an extensive list of references). Better understanding of the Neogene of western Amazonia will require a high-resolution study of multiple sediment cores spanning the entire Neogene sequence throughout the many basins that compose western Amazonia (35). Nevertheless, it is evident that Amazonian landscape has had major changes over the past ~20 Ma. We need to understand those changes across the vast Amazonian landscape, because they must have had a profound effect on the evolution and biogeographic distribution of its ancient and extant biota as well as on the modern and ancient climate of the continent.

MATERIALS AND METHODS
Location of study sites and seismic lines
The first core, Saltarin, is located in the Llanos Basin in eastern Colombia (4.612°N and 70.495°W; 671 m thick) (see Fig. 1, figs. S2 and S3, table S5, and the Supplementary Materials). The second core, 105-AM, is located in the Amazonas/Solimões Basin in northwestern Brazil (4.25°S and 69.93°W; 405 m thick) (see Fig. 1, figs. S2 and S8, table S5, and the Supplementary Materials). We analyzed the sedimentology of both cores together with two-dimensional (2D) seismic lines, the electric logs of 14 wells located between Saltarin and 105-AM, and previously published information on 15 outcrops (17, 22, 36) and one core (see Fig. 2, figs. S2 and S13, tables S5 and S6, and the Supplementary Materials) (21). A total of 1148 km of 2D seismic lines were selected to correlate the two intervals of marine incursions in the Llanos Basin with the intervals of marine incursions in the Amazonas/Solimões Basin (EMI and MMI) (fig. S2 and table S6). Seismic lines selected in the distal Llanos Basin cover the area between the Saltarin well and the northernmost expression of the Vaupés Arch in the subsurface (fig. S13). These seismic lines were analyzed in conjunction with the electric logs of nine wells (fig. S9). In the Amazonas/Solimões Basin, a few seismic lines along major rivers in Colombia and a published seismic line in Brazil (37) allowed us to compare seismic facies between the two basins (figs. S2 and S14); however, there are no wells near those seismic lines that would permit a better integration of seismic facies with stratigraphic units (fig. S10). A total of nine isolated outcrops of Miocene units along river margins, as well as two cores in the Solimões Basin, are the only reference for identification of the uppermost seismic level (fig. S2 and table S5). Analysis was restricted to the Llanos and Amazonas/Solimões basins (fig. S1).

Sedimentology and sequence stratigraphy
The cores Saltarin and 105-AM were described at a scale of 1:50 for identification of grain-sized trends, sedimentary structures, clast composition, thickness of lamination, bioturbation patterns, and macrofossil identification, all of which are used to identify individual lithofacies. The association of lithofacies within a vertical and conformable succession supports the interpretation of depositional environment, following the criteria of James and Dalrymple (38) and Miall (39). Sequence stratigraphy analysis follows the criteria described by Catuneanu et al. (40) for the definition of dominant stacking patterns of deposition (aggradation, progradation, and retrogradation) and bounding surfaces (sequence boundaries and maximum flooding surfaces) that could be used for regional correlation. For fluvial strata, we used the terms "low accommodation" and "high accommodation" system tracts (40). For homogeneous fine-grained strata accumulated in shallow waters, we used a combination of lithofacies and biostratigraphy data to identify the stratigraphic surfaces of correlation. All sedimentological, biostratigraphic, and stratigraphic data are stored and displayed using the SDAR software (41). We grouped depositional settings into three major depositional environments: Continental, Marginal, and Marine. (i) The Continental environment includes interbeds of massive to cross-bedded sandstones and conglomeratic sandstones with a sharp lower contact and light-colored mudstones that can contain sideritic spherulites and nodules. These lithofacies represent accumulation in fluvial channels and adjacent floodplains, with evidence of paleosol development by subaerial exposure. (ii) The Marginal environment includes greenish to gray, laminated, bioturbated, and locally fossil-rich mudstones coarsening up to very fine grained to medium-grained sandstones with coal interbeds. The association of these lithofacies represents accumulation on deltaic plains; low-energy wetlands with swamps, ponds, and channels; and shallow freshwater lacustrine systems. (iii) The Marine environment includes planar-laminated and massive fine-grained lithofacies with high proportions of MPs. In 105-AM, marine lithofacies also include organic matter (peat) and fossil fragments. The content of both MPs (dinoflagellates, marine acritarchs, and foram linings) and macrofossils in those lithofacies supports the marine environment interpretation, yet salinities may have been in part very low, ranging from >5 to up to 30 practical salinity units (36).

Marine intervals
All the analyses, unless noted, were performed using R for Statistical Computing (42). All comparisons are the result of two-sided t tests to evaluate the equality of means in two unpaired samples. P value is reported for each test at the appropriate point in the text, along with degrees of freedom (df) calculated using the Welch modification to account for different variances in the groups being compared. We measured the proportion of terrestrial palynomorphs (pollen and spores), MPs (dinoflagellates, marine acritarchs, and foraminifera linings), and freshwater indicators (*Pediastrum* and *Botryococcus*) in 233 samples, which included 138 samples from Saltarin (1 sample every ~4.7 m) and 95 samples from 105-AM (1 sample every ~3 m). We also measured the BIT index of 18 samples from Saltarin to quantify the input of marine-dwelling Thaumarchaeota versus soil bacteria. Two marine macrofossils found in Saltarin were described and identified. Pollen samples were prepared following standard palynological techniques of digesting sediments in mineral acids (HF and HCl), alkaline treatment in KOH, heavy liquid separation using $ZnBr_2$, and sieving (43). We used panning rather than centrifugation to avoid breaking apart fragile palynomorphs (for example, foram linings). Samples were processed at the laboratory of Paleoflora, Bucaramanga, Colombia. At least 300 palynomorph grains were counted per sample when possible. Palynomorphs were grouped into three broad categories: terrestrial palynomorphs (pollen and spores), MPs (dinoflagellate cysts, marine acritarchs, and foram linings), and freshwater algae indicators (*Pediastrum* and *Botryococcus*). These groups have been used extensively to distinguish continental, marine, and large-lake sequences (43–48). The proportion of the sum of MPs and freshwater algae indicators (lacustrine) relative to the total sum of each sample was calculated. Samples with counts lower than 100 grains were excluded from the analysis. The BIT index is a proxy for the input of soil and riverine organic matter in marine environments [see the study of Schouten et al. (30) and references therein]. We measured the BIT index of 18 samples from Saltarin to quantify the input of

marine-dwelling Thaumarchaeota versus soil bacteria following the standard technique of Schouten *et al.* (*49*) (see the Supplementary Materials).

Paleogeographic reconstruction

The construction of 30 paleogeographic maps illustrates the extension of Continental, Marginal, and Marine environments from ~18.4 to ~10.5 Ma. The source of the dating is discussed in the next section. This quantified and age-controlled reconstruction of the temporal and spatial change of depositional environments and illustration of the extension of marine incursions was carried out in the open-source software GPlates (see file S1) (*50*). This software uses the state-of-the-art global plate reconstruction models, although accumulation occurs in a minor deformed segment of the Andean foreland and intracratonic basins. We used the global coastline and plate movement of South American craton of GPlates (*51*) as the base information to load our geological data (wells, outcrop localities, and seismic lines) and the interpretation of (i) boundaries among nondeposition, Continental, Marginal, and Marine environments; (ii) location of northern Andes deformation front [modified from Reyes-Harker *et al.* (*52*)]; (iii) interpreted location of depositional boundary along the Guiana Shield; and (iv) location of intrabasinal uplifts. Paleogeographic reconstructions of the marine intervals over the Marginal and Continental environments used (i) lithological associations of strata bounded by stratigraphic surfaces of correlations in the two analyzed wells (Saltarin and 105-AM), which have detailed age control; (ii) lithological control on the nine wells in the Llanos Basin, two wells with palynological report of marine influence (*53*), and one well in the Solimões Basin; (iii) palynological control and sedimentological analysis on nine outcrops of the Colombian Amazonas published in the literature; (iv) location of the northern Andes deformation front for middle and late Miocene (*52*); (v) provenance analysis from Hoorn (*22*) and Salamanca Villegas *et al.* (*19*) for the Amazonas outcrop sections, as well as from Bayona *et al.* (*54*) for the Saltarin well; (vi) location of internal uplifts in the Llanos Basin based on seismic information, as well as location of regional structural highs, such as the Vaupés Arch, Baúl High, and Macarena Range (see section S4.1); and (vii) present extent of Miocene strata on the Guiana Shield.

Chronology of cores

Dating and correlation of the two cores were done using sequence stratigraphy together with graphic correlation (*55*) of palynological data using a biostratigraphic zonation for the region that is calibrated with magnetostratigraphy, carbon isotopes, and foraminifera (*56*). We also measured the organic carbon stable isotope value in 118 samples from Saltarin and 71 samples from 105-AM and analyzed the mollusk fauna found in 105-AM to calibrate age determinations. Isolated outcrops reported in the literature were also used to establish the extent of any possible marine event. We used graphic correlation to analyze the palynological information. Graphic correlation (*55, 57, 58*) has been extensively used over the past decades in multiple studies (*56, 59–61*). It does not make the a priori assumption that first and last appearance data in a section record speciation and extinction events. It combines the information of multiple sections to find the true stratigraphic range of a taxon; therefore, the use of an "index" fossil is not necessary because the whole assemblage is being compared. The graphic correlation analysis was done using GraphCor (*62*), and it was applied to the records of both Saltarin and 105-AM. We used the standard composite section of Jaramillo *et al.* (*56*). Three rounds of correlation were performed until the line of correlation (LOC) for each section became stable.

Derived from both LOCs of this first step, a LOC between Saltarin and 105-AM was produced. Sequence stratigraphic events were added to this LOC to improve the correlation in between the data provided by biostratigraphy (Fig. 1). The modified LOC of Saltarin versus 105-AM was then extrapolated to the LOC of both sections versus the composite. The new LOC lines were reevaluated using the biostratigraphic data. This process was repeated for several rounds until the LOCs of both Saltarin versus composite, 105-AM versus composite, and Saltarin versus 105-AM were stable.

To transfer the stratigraphic position of each sample in the two well cores from meters to geologic time, we assumed a linear sedimentation rate between the points in the LOC. It is reasonable to assume linearity because the composite does not have major stratigraphic breaks. The calibration of Jaramillo *et al.* (*56*) was used, and the R (*42*) code used for the process can be found in file S2. The geological time scale follows Gradstein *et al.* (*63*) and Hilgen *et al.* (*64*). It is important to stress that ages provided in this research are relative, and the precision goes as far as the calibration points for the zonation. Ages between calibration points are derived from linear interpolation. Therefore, we do not argue that our ages are precisely calibrated with the geological time record, but they indicate a relative age compared to sediments above and below. These ages represent a hypothesis, and it is based on the best information we have at the moment; they could change as more calibration points are added to the zonation or if a calibration point is shifted or the LOC of each section is modified. Our ages are fully replicable, as we provide the LOC, the full zonation, and the calibration points. Stable carbon isotopes were used to support the age determinations produced by the graphic correlation analysis. Stable carbon isotope values of bulk organic matter ($\delta^{13}C_{OM}$) were measured via flash combustion at 1020°C in a Costech elemental analyzer fitted to a Thermo Finnigan DELTAplus XL isotope ratio mass spectrometer (Department of Geological Sciences, University of Florida). Carbonate present in the samples was removed by digestion using 1.0 N HCl. Analytical precision and accuracy were determined by repeated analysis of the USGS40 standard. Overall uncertainty was better than 0.08‰. Organic carbon content (total organic carbon) was determined on the basis of measurement of total carbon by combustion using a Carlo Erba elemental analyzer minus total inorganic carbon measured by acidification using the AutoMate Prep Device coupled to the UIC 5011 CO_2 Coulometer.

SUPPLEMENTARY MATERIALS

Supplementary material for this article is available at http://advances.sciencemag.org/cgi/content/full/3/5/e1601693/DC1

section S1. General information
section S2. Sedimentology and sequence stratigraphy analyses
section S3. Marine intervals
section S4. Basin-wide correlations
section S5. Chronology of cores
section S6. Sites from the literature used in this study
section S7. Other published sites beyond the boundaries of this study
fig. S1. Map of northwestern South America showing the sedimentary basins discussed in the text and the structural features that divide them.
fig. S2. Location of the nine wells in the Llanos Basin, two wells in the Amazonas/Solimões Basin, and 13 seismic lines used for this study (geographic coordinates in tables S5 and S6).
fig. S3. Sedimentological and sequence stratigraphic interpretation of the Saltarin well (see details of interpretation in table S7).
fig. S4. Graphic correlation of Saltarin versus 105-AM using geological time as scale in both axes, rather than stratigraphic thickness.
fig. S5. Photomicrographs of selected dinoflagellate cysts and acritarchs.
fig. S6. Carchariniformes gen. et sp. indet. tooth from the core Saltarin, Carbonera C2 Formation, early Miocene, 630.08 m, specimen MUN STRI-40967.

fig. S7. Dactyl of raptorial appendage (second thoracopod) of a fossil mantis shrimp from the Carbonera Formation, early Miocene, Colombia, MUN STRI-40281.

fig. S8. Sedimentological and sequence stratigraphic interpretation of the 105-AM well (see details of interpretation in table S8).

fig. S9. Stratigraphic correlation of the two major marine incursions (EMI and MMI) from the Saltarin well to the northernmost expression of the Vaupés Arch in the subsurface (well I).

fig. S10. Stratigraphic correlation of the two major marine incursions (EMI and MMI) along the northern Amazonas/Solimões Basin.

fig. S11. Graphic correlation between the standard composite section of Jaramillo et al. (56) and core Saltarin.

fig. S12. Graphic correlation between the standard composite section of Jaramillo et al. (56) and core 105-AM.

fig. S13. Seismic profiles in the Llanos Basin (see location in fig. S2; interpretation only at one extreme of the line) illustrate the seismic facies of the two marine incursions (EMI and MMI).

fig. S14. Interpreted 2D seismic profiles showing the contrasting difference of seismic facies between undifferentiated Cenozoic and Cretaceous units in the Amazonas/Solimões Basin (see fig. S2 for the location of seismic lines).

fig. S15. Graphic correlation between the cores Saltarin and 105-AM.

fig. S16. Carbon isotope data (δ13C) versus stratigraphic position in core Saltarin on the left panel.

fig. S17. Carbon isotope data (δ13C) versus stratigraphic position in core 105-AM.

fig. S18. Photographs of shells from core 105-AM.

fig. S19. Molluscan biostratigraphy of core 105-AM.

table S1. Palynomorph counts for samples analyzed in core Saltarin.

table S2. Palynomorph counts for samples analyzed in core 105-AM.

table S3. Summary of palynological count data.

table S4. BIT index for Saltarin samples.

table S5. Geographic coordinates and information of outcrops and wells (coordinate system WGS 1984) used in this study.

table S6. Geographic coordinates and information of 2D seismic lines (coordinate system WGS 1984) used in this study.

table S7. Summary of lithological and palynological indicators for depositional environment interpretation of the Saltarin well.

table S8. Summary of lithological and palynological indicators for the depositional environment interpretation of the 105-AM well.

table S9. LOC data points for Saltarin versus composite, 105-AM versus composite, and 105-AM versus Saltarin.

table S10. Age of individual samples derived from the graphic correlation analysis.

table S11. Total carbon, total inorganic carbon, total organic carbon, total nitrogen, and carbon isotope data for all studied samples.

table S12. Mollusks identified in core 105-AM.

file S1. GPlates project.

file S2. R code.

file S3. Graphic correlation.

file S4. Biostratigraphic and sequence stratigraphic events.

file S5. Lithological description of the cores 105-AM and Saltarin.

file S6. Excel tables.

References (65–134, 138–185)

REFERENCES AND NOTES

1. C. Hoorn, F. P. Wesselingh, H. ter Steege, M. A. Bermudez, A. Mora, J. Sevink, I. Sanmartín, A. Sanchez-Meseguer, C. L. Anderson, J. P. Figueiredo, C. Jaramillo, D. Riff, F. R. Negri, H. Hooghiemstra, J. Lundberg, T. Stadler, T. Särkinen, A. Antonelli, Amazonia through time: Andean uplift, climate change, landscape evolution and biodiversity. Science 330, 927–931 (2010).

2. N. R. Lovejoy, J. S. Albert, W. G. R. Crampton, Miocene marine incursions and marine/freshwater transitions: Evidence from Neotropical fishes. J. South Am. Earth Sci. 21, 5–13 (2006).

3. F. P. Wesselingh, C. Hoorn, S. B. Kroonenberg, A. Antonelli, J. G. Lundberg, H. B. Vonhof, H. Hooghiemstra, in Amazonia, Landscape and Species Evolution: A Look into the Past, C. Hoorn, F. P. Wesselingh, Eds. (Wiley-Blackwell, 2010), pp. 421–431.

4. S. D. Webb, Biological implications of the middle Miocene Amazon seaway. Science 269, 361–362 (1995).

5. N. R. Lovejoy, R. E. Bermingham, A. P. Martin, Marine incursions into South America. Nature 396, 421–422 (1998).

6. H. Hamilton, S. Caballero, A. G. Collins, R. L. Brownell Jr., Evolution of river dolphins. Proc. R. Soc. B 268, 549–556 (2001).

7. M. Iriondo, Large wetlands of South America: A model for Quaternary humid environments. Quat. Int. 114, 3–9 (2004).

8. T. Toivonen, S. Mäki, R. Kalliola, The riverscape of Western Amazonia—A quantitative approach to the fluvial biogeography of the region. J. Biogeogr. 34, 1374–1387 (2007).

9. J. Terborgh, E. Andresen, The composition of Amazonian forests: Patterns at local and regional scales. J. Trop. Ecol. 14, 645–664 (1998).

10. E. M. Latrubesse, M. Cozzuol, S. A. F. da Silva-Caminha, C. A. Rigsby, M. L. Absy, C. Jaramillo, The late Miocene paleogeography of the Amazon Basin and the evolution of the Amazon River system. Earth Sci. Rev. 99, 99–124 (2010).

11. G. E. Shephard, R. D. Müller, L. Liu, M. Gurnis, Miocene drainage reversal of the Amazon River driven by plate–mantle interaction. Nat. Geosci. 3, 870–875 (2010).

12. E. M. Latrubesse, S. A. F. da Silva, M. Cozzuol, M. L. Absy, Late Miocene continental sedimentation in southwestern Amazonia and its regional significance: Biotic and geological evidence. J. South Am. Earth Sci. 23, 61–80 (2007).

13. F. P. Wesselingh, J. Guerrero, M. E. Räsänen, L. R. Pittmann, H. B. Vonhof, Landscape evolution and depositional processes in the Miocene Amazonian Pebas lake/wetland system: Evidence from exploratory boreholes in northeastern Peru. Scr. Geol. 133, 323–363 (2006).

14. K. E. Campbell Jr., C. D. Frailey, L. R. Pitman, The Pan-Amazonian Ucayali peneplain, late Neogene sedimentation in Amazonia, and the birth of the modern Amazon River system. Palaeogeogr. Palaeoclimatol. Palaeoecol. 239, 166–219 (2006).

15. M. A. Cozzuol, The Acre vertebrate fauna: Age, diversity, and geography. J. South Am. Earth Sci. 21, 185–203 (2006).

16. C. D. Frailey, E. L. Lavina, A. Rancy, J. P. de Souza-Filho, A proposed Pleistocene/Holocene lake in the Amazon basin and its significance to Amazonian Geology and biogeography. Acta Amazon. 18, 119–143 (1988).

17. C. Hoorn, Fluvial palaeoenvironments in the intracratonic Amazonas Basin (early Miocene–early middle Miocene, Colombia). Palaeogeogr. Palaeoclimatol. Palaeoecol. 109, 1–54 (1994).

18. J. Hovikoski, M. Gingras, M. Räsänen, L. A. Rebata, J. Guerrero, A. Ranzi, J. Melo, L. Romero, H. Nuñez del Prado, F. Jaimes, S. Lopez, The nature of Miocene Amazonian epicontinental embayment: High-frequency shifts of the low-gradient coastline. Geol. Soc. Am. Bull. 119, 1506–1520 (2007).

19. S. Salamanca Villegas, E. E. van Soelen, M. L. Teunissen van Manen, S. G. A. Flantua, R. Ventura Santos, M. Roddaz, E. L. Dantas, E. van Loon, J. S. S. Damsté, J.-H. Kim, C. Hoorn, Amazon forest dynamics under changing abiotic conditions in the early Miocene (Colombian Amazonia). J. Biogeogr. 43, 2424–2437 (2016).

20. M. Räsänen, A. M. Linna, J. C. R. Santos, F. R. Negri, Late Miocene tidal deposits in the Amazonian foreland basin. Science 269, 386–389 (1995).

21. C. Hoorn, Marine incursions and the influence of Andean tectonics on the Miocene depositional history of northwestern Amazonia: Results of a palynostratigraphic study. Palaeogeogr. Palaeoclimatol. Palaeoecol. 105, 267–309 (1993).

22. C. Hoorn, An environmental reconstruction of the palaeo-Amazon River system (middle-late Miocene, NW Amazonia). Palaeogeogr. Palaeoclimatol. Palaeoecol. 112, 187–238 (1994).

23. C. Hoorn, Mangrove forests and marine incursions in Neogene Amazonia (Lower Apaporis River, Colombia). Palaios 21, 197–209 (2006).

24. J. Hovikoski, F. P. Wesselingh, M. Räsänen, M. Gingras, H. Vonhof, in Amazonia, Landscape and Species Evolution: A Look into the Past, C. Hoorn, F. P. Wesselingh, Eds. (Wiley-Blackwell, 2010), pp. 143–161.

25. E. M. Latrubesse, J. Bocquentin, J. C. R. Santos, C. G. Ramonell, Paleoenvironmental model for the late Cenozoic southwestern Amazonia: Paleontology and geology. Acta Amazon. 27, 103–118 (1997).

26. F. P. Wesselingh, J. A. Salo, A Miocene perspective on the evolution of the Amazonian biota. Scr. Geol. 133, 439–458 (2006).

27. F. P. Wesselingh, M. E. Räsänen, G. Irion, H. B. Vonhot, R. Kaandorp, W. Renema, L. Romero Pittman, M. Gringas, Lake Pebas: A palaeoecological reconstruction of a Miocene, long-lived lake complex in western Amazonia. Cainozoic Res. 1, 35–81 (2002).

28. M. Roddaz, S. Brusset, P. Baby, G. Hérail, Miocene tidal-influenced sedimentation to continental Pliocene sedimentation in the forebulge–backbulge depozones of the Beni–Mamore foreland Basin (northern Bolivia). J. South Am. Earth Sci. 20, 351–368 (2006).

29. H. B. Vonhof, F. P. Wesselingh, R. J. G. Kaandorp, G. R. Davies, J. E. van Hinte, J. Guerrero, M. Räsänen, L. Romero-Pittman, A. Ranzi, Paleogeography of Miocene Western Amazonia: Isotopic composition of molluscan shells constrains the influence of marine incursions. Geol. Soc. Am. Bull. 115, 983–993 (2003).

30. S. Schouten, E. C. Hopmans, J. S. Sinninghe Damsté, The organic geochemistry of glycerol dialkyl glycerol tetraether lipids: A review. Org. Geochem. 54, 19–61 (2013).

31. C. Zell, J.-H. Kim, G. Abril, R. L. Sobrinho, D. Dorhout, P. Moreira-Turcq, J. S. Sinninghe Damsté, Impact of seasonal hydrological variation on the distributions of tetraether lipids along the Amazon River in the central Amazon basin: Implications for the MBT/CBT paleothermometer and the BIT index. Front. Microbiol. 4, 228 (2013).

32. L. J. V. Compagno, M. Dando, S. L. Fowler, *Sharks of the World* (Princeton Univ. Press, 2005).

33. H. Dingle, R. L. Caldwell, Ecology and morphology of feeding and agonistic behavior in mudflat stomatopods (Squillidae). *Biol. Bull.* **155**, 134–149 (1978).

34. A. Mora, P. Baby, M. Roddaz, M. Parra, S. Brusset, W. Hermoza, N. Espurt, in *Amazonia, Landscape and Species Evolution: A Look into the Past,* C. Hoorn, F. P. Wesselingh, Eds. (Wiley-Blackwell, 2010), pp. 38–60.

35. P. A. Baker, S. C. Fritz, C. G. Silva, C. A. Rigsby, M. L. Absy, R. P. Almeida, M. Caputo, C. M. Chiessi, F. W. Cruz, C. W. Dick, S. J. Feakins, J. Figueiredo, K. H. Freeman, C. Hoorn, C. Jaramillo, A. K. Kern, E. M. Latrubesse, M. P. Ledru, A. Marzoli, A. Myrbo, A. Noren, W. E. Piller, M. I. F. Ramos, C. C. Ribas, R. Trnadade, A. J. West, I. Wahnfried, D. A. Willard, Trans-Amazon Drilling Project (TADP): Origins and evolution of the forests, climate, and hydrology of the South American tropics. *Sci. Drill.* **20**, 41–49 (2015).

36. M. Boonstra, M. I. F. Ramos, E. I. Lammertsma, P.-O. Antoine, C. Hoorn, Marine connections of Amazonia: Evidence from foraminifera and dinoflagellate cysts (early to middle Miocene, Colombia/Peru). *Palaeogeogr. Palaeoclimatol. Palaeoecol.* **417**, 176–194 (2015).

37. A. R. A. Costa, thesis, Universidade Federal do Pará (2002).

38. N. P. James, R. W. Dalrymple, *Facies Models 4* (GEOtext 6, The Geological Association of Canada, 2010), 586 pp.

39. A. D. Miall, *The Geology of Fluvial Deposits: Sedimentary Facies, Basin Analysis, and Petroleum Geology* (Springer, 1996), 582 pp.

40. O. Catuneanu, V. Abreu, J. P. Bhattacharya, M. D. Blum, R. W. Dalrymple, P. G. Eriksson, C. R. Fielding, W. L. Fisher, W. E. Galloway, M. R. Gibling, K. A. Giles, J. M. Holbrook, R. Jordan, C. G. S. C. Kendall, B. Macurda, O. J. Martinsen, A. D. Miall, J. E. Neal, D. Nummedal, L. Pomar, H. W. Posamentier, B. R. Pratt, J. F. Sarg, K. W. Shanley, R. J. Steel, A. Strasser, M. E. Tucker, C. Winker, Towards the standardization of sequence stratigraphy. *Earth Sci. Rev.* **92**, 1–33 (2009).

41. J. Ortiz, C. Moreno, A. Cardenas, C. Jaramillo, SDAR 1.0 a new quantitative toolkit for analyze stratigraphic data. *Geophys. Res. Abstr.* **17**, EGU2015–EGU2790 (2015).

42. R Development Core Team, "R: A language and environment for statistical computing" (R Foundation for Statistical Computing, 2013); www.R-project.org.

43. A. Traverse, *Paleopalynology* (Springer, ed. 2, 2007), 813 pp.

44. M. A. Lorente, *Palynology and Palynofacies of the Upper Tertiary in Venezuela* (J. Cramer, 1986), 222 pp.

45. J. Muller, Palynology of Recent Orinoco delta and shelf sediments: Reports of the Orinoco shelf expedition. *Micropaleontology* **5**, 1–32 (1959).

46. C.-C. Hofmann, Pollen distribution in sub-recent sedimentary environments of the Orinoco Delta (Venezuela)—An actuo-palaeobotanical study. *Rev. Palaeobot. Palynol.* **119**, 191–217 (2002).

47. C. Santos, C. Jaramillo, G. Bayona, M. Rueda, V. Torres, Late Eocene marine incursion in north-western South America. *Palaeogeogr. Palaeoclimatol. Palaeoecol.* **264**, 140–146 (2008).

48. V. Rull, Sequence analysis of western Venezuelan Cretaceous to Eocene sediments using palynology: Chronopaleoenvironmental and paleovegetational approaches. *Palynology* **21**, 79–90 (1997).

49. S. Schouten, C. Huguet, E. C. Hopmans, M. V. M. Kienhuis, J. S. Sinninghe-Damsté, Analytical methodology of the TEX$_{86}$ paleothermometry by high-performance liquid chromatography/atmospheric pressure chemical ionization–mass spectrometry. *Anal. Chem.* **79**, 2940–2944 (2007).

50. J. A. Boyden, R. D. Müller, M. Gurnis, T. H. Torsvik, J. A. Clark, M. Turner, H. Ivey-Law, R. J. Watson, J. S. Cannon, in *Geoinformatics: Cyberinfrastructure for the Solid Earth Sciences,* G. R. Keller, C. Baru, Eds. (Cambridge Univ. Press, 2011), pp. 95–113.

51. M. Seton, R. D. Müller, S. Zahirovic, C. Gaina, T. Torsvik, G. Shephard, A. Talsma, M. Gurnis, M. Turner, S. Maus, M. Chandler, Global continental and ocean basin reconstructions since 200 Ma. *Earth Sci. Rev.* **113**, 212–270 (2012).

52. A. Reyes-Harker, C. F. Ruiz-Valdivieso, A. Mora, J. C. Ramírez-Arias, G. Rodriguez, F. de la Parra, V. Caballero, M. Parra, N. Moreno, B. K. Horton, J. E. Saylor, A. Silva, V. Valencia, D. Stockli, V. Blanco, Cenozoic paleogeography of the Andean foreland and retroarc hinterland of Colombia. *Am. Assoc. Pet. Geol. Bull.* **99**, 1407–1453 (2015).

53. G. Bayona, C. Jaramillo, M. Rueda, A. Reyes-Harker, V. Torres, Paleocene-middle Miocene flexural-margin migration of the nonmarine Llanos foreland basin of Colombia. *CTF Cienc. Tecnol. Futuro* **3**, 141–160 (2007).

54. G. Bayona, A. Valencia, A. Mora, M. Rueda, J. Ortiz, O. Montenegro, Stratigraphy and provenance of Miocene rocks in the distal Llanos foreland basin of Colombia. *Geol. Colomb.* **33**, 23–46 (2008).

55. L. E. Edwards, Supplemented graphic correlation: A powerful tool for paleontologists and nonpaleontologists. *Palaios* **4**, 127–143 (1989).

56. C. A. Jaramillo, M. Rueda, V. Torres, A palynological zonation for the Cenozoic of the Llanos and Llanos Foothills of Colombia. *Palynology* **35**, 46–84 (2011).

57. L. E. Edwards, Insights on why graphic correlation (Shaw's method) works. *J. Geol.* **92**, 583–597 (1984).

58. A. B. Shaw, *Time in Stratigraphy* (McGraw-Hill, 1964), 365 pp.

59. K. O. Mann, H. R. Lane, in *Graphic Correlation,* K. O. Mann, H. R. Lane, P. A. Scholle, Eds., vol. 53 of *SEPM Special Publication* (SEPM Society For Sedimentary Geology, 1995), pp. 3–13.

60. J. L. Carney, R. W. Pierce, in *Graphic Correlation,* K. O. Mann, H. R. Lane, P. A. Scholle, Eds., vol. 53 of *SEPM Special Publication* (SEPM Society For Sedimentary Geology, 1995), pp. 23–43.

61. R. A. Cooper, J. S. Crampton, J. I. Raine, F. M. Gradstein, H. E. G. Morgans, P. M. Sadler, C. P. Strong, D. Waghorn, G. J. Wilson, Quantitative biostratigraphy of the Taranaki Basin, New Zealand: A deterministic and probabilistic approach. *Am. Assoc. Pet. Geol. Bull.* **85**, 1469–1498 (2001).

62. K. C. Hood, *GraphCor—Interactive Graphic Correlation Software* (Kenneth C. Hood, 1998).

63. F. M. Gradstein, J. G. Ogg, M. D. Schmitz, G. M. Ogg, Eds., *The Geologic Time Scale 2012* (Elsevier, 2012), vol. 2.

64. F. J. Hilgen, L. J. Lourens, J. A. Van Dam, A. G. Beu, A. F. Boyes, R. A. Cooper, W. Krijgsman, J. G. Ogg, W. E. Piller, D. S. Wilson, in *The Geologic Time Scale 2012,* F. M. Gradstein, J. G. Ogg, M. D. Schmitz, G. M. Ogg, Eds. (Elsevier, 2012), pp. 923–978.

65. S. Silva-Caminha, C. Jaramillo, M. L. Absy, Neogene palynology of the Solimões basin, Brazilian Amazonia. *Palaeontogr. Abt. B* **283**, 1–67 (2010).

66. J. Hovikoski, M. Räsänen, M. Gingras, A. Ranzi, J. Melo, Tidal and seasonal controls in the formation of late Miocene inclined heterolithic stratification deposits, western Amazonian foreland basin. *Sedimentology* **55**, 499–530 (2008).

67. R. Westaway, Late Cenozoic sedimentary sequences in Acre state, southwestern Amazonia: Fluvial or tidal? Deductions from the IGCP 449 fieldtrip. *J. South Am. Earth Sci.* **21**, 120–134 (2006).

68. J. Hovikoski, M. Räsänen, M. Gingras, M. Roddaz, S. Brusset, W. Hermoza, L. Romero Pittman, K. Lertola, Miocene semidiurnal tidal rhythmites in Madre de Dios, Peru. *Geology* **33**, 177–180 (2005).

69. L. A. Rebata-H, M. K. Gingras, M. E. Räsänen, M. Barberi, Tidal-channel deposits on a delta plain from the Upper Miocene Nauta Formation, Marañón Foreland Sub-basin, Peru. *Sedimentology* **53**, 971–1013 (2006).

70. L. A. Rebata-H, M. E. Räsänen, M. K. Gingras, V. Vieira Jr., M. Barberi, G. Irion, Sedimentology and ichnology of tide-influenced Late Miocene successions in western Amazonia: The gradational transition between the Pebas and Nauta formations. *J. South Am. Earth Sci.* **21**, 96–119 (2006).

71. F. P. Wesselingh, M. M. C. van der Hoorn, J. Guerrero, M. Räsänen, L. Romero-Pitmann, J. A. Salo, The stratigraphy and regional structure of Miocene deposits in western Amazonia (Peru, Colombia and Brazil), with implications for late Neogene landscape evolution. *Scr. Geol.* **133**, 291–322 (2006).

72. M. K. Gingras, M. Räsänen, S. G. Pemberton, L. P. Romero, Ichnology and sedimentology reveal depositional characteristics of bay-margin parasequences in the Miocene Amazonian foreland basin. *J. Sediment. Res.* **72**, 871–883 (2002).

73. R. Hernández, T. E. Jordan, A. D. Farjat, L. Echavarría, B. D. Idleman, J. H. Reynolds, Age, distribution, tectonics, and eustatic controls of the Paranense and Caribbean marine transgressions in southern Bolivia and Argentina. *J. South Am. Earth Sci.* **19**, 495–512 (2005).

74. M. E. Räsänen, A. Linna, G. Irion, L. R. Hernani, R. V. Huaman, F. Wesselingh, in *Geoecología y Desarrollo Amazónico: Estudio Integrado en la Zona de Iquitos, Perú,* R. Kalliola, S. Flores-Paitan, Eds. (Annales Universitatis Turkuensis Series A II, Turun Yliopisto, 1998), pp. 59–137.

75. M. E. Räsänen, J. S. Salo, R. J. Kalliola, Fluvial perturbance in the western Amazon basin: Regulation by long-term sub-Andean tectonics. *Science* **238**, 1398–1401 (1987).

76. C. Hoorn, M. Roddaz, R. Dino, E. Soares, C. Uba, D. Ochoa-Lozano, R. Mapes, in *Amazonia, Landscape and Species Evolution: A Look into the Past,* C. Hoorn, F. P. Wesselingh, Eds. (Wiley-Blackwell, 2010), pp. 103–122.

77. C. Hoorn, F. P. Wesselingh, J. Hovikoski, J. Guerrero, in *Amazonia, Landscape and Species Evolution: A Look into the Past,* C. Hoorn, F. P. Wesselingh, Eds. (Wiley-Blackwell, 2010), pp. 123–142.

78. D. F. Rossetti, M. C. L. Cohen, S. H. Tatumi, A. O. Sawakuchi, É. H. Cremon, J. C. R. Mittani, T. C. Bertani, C. J. A. S. Munita, D. R. G. Tudela, M. Yee, G. Moya, Mid-Late Pleistocene OSL chronology in western Amazonia and implications for the transcontinental Amazon pathway. *Sediment. Geol.* **330**, 1–15 (2015).

79. M. Gross, W. E. Piller, M. I. Ramos, J. D. da Silva Paz, Late Miocene sedimentary environments in south-western Amazonia (Solimões Formation; Brazil). *J. South Am. Earth Sci.* **32**, 169–181 (2011).

80. M. Gross, M. I. Ramos, M. Caporaletti, W. E. Piller, Ostracods (Crustacea) and their palaeoenvironmental implication for the Solimões Formation (late Miocene; Western Amazonia/Brazil). *J. South Am. Earth Sci.* **42**, 216–241 (2013).

81. A. P. Linhares, M. I. F. Ramos, M. Gross, W. E. Piller, Evidence for marine influx during the Miocene in southwestern Amazonia, Brazil. *Geol. Colomb.* **36**, 91–104 (2011).

82. F. P. Wesselingh, M. I. F. Ramos, in *Amazonia, Landscape and Species Evolution: A Look into the Past,* C. Hoorn, F. P. Wesselingh, Eds. (Wiley-Blackwell, 2010), pp. 302–316.

83. G. Vermeij, F. Wesselingh, Neogastropod molluscs from the Miocene of western Amazonia, with comments on marine to freshwater transitions in molluscs. *J. Paleontol.* **76**, 265–270 (2002).

84. F. P. Wesselingh, Molluscs from the Miocene Pebas Formation of Peruvian and Colombian Amazonia. *Scr. Geol.* **133**, 19–290 (2006).

85. F. P. Wesselingh, Miocene long-lived lake Pebas as a stage of mollusk radiations, with implications for landscape evolution in western Amazonia. *Scr. Geol.* **133**, 1–17 (2006).

86. F. P. Wesselingh, R. J. G. Kaandorp, H. B. Vonhof, M. E. Räsänen, W. Renema, M. Gingras, The nature of aquatic landscapes in the Miocene of western Amazonia: An integrated palaeontological and geochemical approach. *Scr. Geol.* **133**, 363–393 (2006).

87. F. P. Wesselingh, O. Macsotay, *Pachydon hettneri* (Anderson, 1928) as indicator for Caribbean–Amazonian lowland connections during the early–middle Miocene. *J. South Am. Earth Sci.* **21**, 49–53 (2006).

88. F. A. Muñoz-Torres, R. C. Whatley, D. van Harten, Miocene ostracod (Crustacea) biostratigraphy of the upper Amazon Basin and evolution of the genus *Cyprideis*. *J. South Am. Earth Sci.* **21**, 75–86 (2006).

89. F. A. Muñoz-Torres, R. C. Whatley, D. van Harten, The endemic nonmarine Miocene ostracod fauna of the upper Amazon Basin. *Rev. Española de Micropaleontol.* **30**, 89–105 (1998).

90. M. Gross, M. I. F. Ramos, W. E. Piller, On the Miocene *Cyprideis* species flock (Ostracoda; Crustacea) of Western Amazonia (Solimões Formation): Refining taxonomy on species level. *Zootaxa* **3899**, 1–69 (2014).

91. M. Gross, M. I. F. Ramos, W. E. Piller, A minute ostracod (Crustacea: Cytheromatidae) from the Miocene Solimões Formation (western Amazonia, Brazil): Evidence for marine incursions? *J. Syst. Palaeontol.* **14**, 581–602 (2016).

92. W. M. Gabb, Descriptions of fossils from the clay deposits of the upper Amazon. *Am. J. Conchol.* **4**, 197–200 (1869).

93. T. A. Conrad, Remarks on the Tertiary clay of the upper Amazon, with descriptions of new shells. *Proc. Acad. Nat. Sci. Philadelphia* **26**, 25–32 (1874).

94. R. Etheridge, Notes on the Mollusca collected by C. Barrington Brown, Esq., A.R.S.M., from the Tertiary deposits of Solimões and Javary Rivers, Brazil. *Quart. J. Geol. Soc. Lond.* **35**, 82–88 (1879).

95. C. D. Frailey, Late Miocene and Holocene mammals, exclusive of the Notoungulata, of the Rio Acre region, western Amazonia. *Contrib. Sci.* **374**, 1–46 (1986).

96. K. A. Monsch, Miocene fish faunas from the northwestern Amazonia basin (Colombia, Peru, Brazil) with evidence of marine incursions. *Palaeogeogr. Palaeoclimatol. Palaeoecol.* **143**, 31–50 (1998).

97. C. de Paula Couto, in *II Congreso Latino-Americano de Paleontologia* (Universidade Federal do Rio Grande do Sul, 1981), pp. 461–477.

98. J. V. Tejada-Lara, R. Salas-Gismondi, F. Pujos, P. Baby, M. Benammi, S. Brusset, D. De Franceschi, N. Espurt, M. Urbina, P.-O. Antoine, Life in proto-Amazonia: Middle Miocene mammals from the Fitzcarrald Arch (Peruvian Amazon). *Palaeontology* **58**, 341–378 (2015).

99. R. Salas-Gismondi, J. J. Flynn, P. Baby, J. V. Tejada-Lara, F. P. Wesselingh, P.-O. Antoine, A Miocene hyperdiverse crocodylian community reveals peculiar trophic dynamics in proto-Amazonian mega-wetlands. *Proc. Biol. Sci.* **282**, 20142490 (2015).

100. R. Salas-Gismondi, P.-O. Antoine, P. Baby, S. Brusset, M. Benammi, N. Espurt, D. de Franceschi, F. Pujos, J. Tejada, M. Urbina, Middle Miocene crocodiles from the Fitzcarrald Arch, Amazonian Peru. *Cuadernos del Museo Geominero* **8**, 355–360 (2007).

101. P.-O. Antoine, R. Salas-Gismondi, P. Baby, M. Benammi, S. Brusset, D. Franceshi, N. Espurt, C. Goillot, F. Pujos, J. Tejada, M. Urbina, The middle Miocene (Laventan) Fitzcarraff fauna, Amazonian Peru. *Cuadernos del Museo Geominero* **8**, 19–24 (2007).

102. R. Salas-Gismondi, P. Baby, P.-O. Antoine, F. Pujos, M. Benammi, N. Espurt, S. Brusset, M. Urbina, D. De Franceschi, in *XIII Congreso Peruano de Geología* (Sociedad Geológica del Perú, 2006), pp. 643–646.

103. G. Bianucci, O. Lambert, R. Salas-Gismondi, J. Tejada, F. Pujos, M. Urbina, P.-O. Antoine, A Miocene relative of the Ganges River Dolphin (Odontoceti, Platanistidae) from the Amazonian basin. *J. Vertebr. Paleontol.* **33**, 741–745 (2013).

104. R. J. G. Kaandorp, H. B. Vonhof, F. P. Wesselingh, L. Romero Pittman, D. Kroon, J. E. van Hinte, Seasonal Amazonian rainfall variation in the Miocene Climate Optimum. *Palaeogeogr. Palaeoclimatol. Palaeoecol.* **221**, 1–6 (2005).

105. R. J. G. Kaandorp, F. P. Wesselingh, H. B. Vonhof, Ecological implications from geochemical records of Miocene Western Amazonian bivalves. *J. South Am. Earth Sci.* **21**, 54–74 (2006).

106. H. B. Vonhof, F. P. Wesselingh, G. M. Ganssen, Reconstruction of the Miocene western Amazonian aquatic system using molluscan isotopic signatures. *Palaeogeogr. Palaeoclimatol. Palaeoecol.* **141**, 85–93 (1998).

107. S. Kroonenberg, C. V. Reeves, in *Petroleum Geology of Colombia,* F. Cediel, Ed. (Agencia Nacional de Hidrocarburos–Fondo Editorial Universidad Eafit, 2011), vol. 16, pp. 17–102.

108. G. Montenegro, M. Barragán, in *Petroleum Geology of Colombia,* F. Cediel, Ed. (Agencia Nacional de Hidrocarburos–Fondo Editorial Universidad Eafit, 2011), vol. 4, pp. 1–15.

109. L. F. Sarmiento-Rojas, in *Petroleum Geology of Colombia,* F. Cediel, G. Ojeda, Eds. (Agencia Nacional de Hidrocarburos–Fondo Editorial Universidad Eafit, 2011), vol. 7, pp. 1–154.

110. H. J. White, R. A. Skopec, F. A. Ramirez, J. A. Rodas, G. Bonilla, Reservoir characteristics of the Hollin and Napo formations, western Oriente basin, Ecuador, in *Petroleum Basins of South America,* A. J. Tankard, S. R. Suárez, H. J. Welsink, Eds., vol. 62 of *AAPG Memoir* (American Association of Petroleum Geologists, 1995), pp. 573–596.

111. M. A. Cooper, F. T. Addison, R. Alvarez, M. Coral, R. H. Graham, A. B. Hayward, S. Howe, J. Martinez, J. Naar, R. Penas, A. J. Pulham, A. Taborda, Basin development and tectonic history of the Llanos Basin, Eastern Cordillera and Middle Magdalena Valley, Colombia. *Am. Assoc. Pet. Geol. Bull.* **79**, 1421–1442 (1995).

112. G. Bayona, M. Cortés, C. Jaramillo, G. Ojeda, J. J. Aristizabal, A. Reyes-Harker, An integrated analysis of an orogen–sedimentary basin pair: Latest Cretaceous–Cenozoic evolution of the linked Eastern Cordillera orogen and the Llanos foreland basin of Colombia. *Geol. Soc. Am. Bull.* **120**, 1171–1197 (2008).

113. M. Parra, A. Mora, C. Jaramillo, M. R. Strecker, E. R. Sobel, L. Quiroz, M. Rueda, V. Torres, Orogenic wedge advance in the northern Andes: Evidence from the Oligo-Miocene sedimentary record of the Medina Basin, Eastern Cordillera, Colombia. *Geol. Soc. Am. Bull.* **121**, 780–800 (2009).

114. M. Parra, A. Mora, E. R. Sobel, M. R. Strecker, R. González, Episodic orogenic front migration in the northern Andes: Constraints from low-temperature thermochronology in the Eastern Cordillera, Colombia. *Tectonics* **28**, TC4004 (2009).

115. G. Bayona, O. Montenegro, A. Cardona, C. Jaramillo, F. Lamus, S. Morón, L. Quiroz, M. C. Ruíz, V. Valencia, M. Parra, D. Stockli, Estratigrafía, procedencia, subsidencia y exhumación de las unidades Paleógenas en el Sinclinal de Usme, sur de la zona axial de la Cordillera Oriental. *Geol. Colomb.* **35**, 5–35 (2010).

116. A. Bande, B. K. Horton, J. C. Ramírez, A. Mora, M. Parra, D. F. Stockli, Clastic deposition, provenance, and sequence of Andean thrusting in the frontal Eastern Cordillera and Llanos foreland basin of Colombia. *Geol. Soc. Am. Bull.* **124**, 59–76 (2011).

117. G. Bayona, M. De Armas, P. Villamarin, A. Mora, E. Gomez, J. Guerrero, I. Leyva, A. Valencia, paper presented at the 2009 AAPG International Conference and Exhibition, Rio de Janeiro, Brazil, 15 to 18 November 2009.

118. G. Bayona et al., in *Memorias del X Simposio Bolivariano de Cuencas Subandinas* (Asociación Colombiana de Geólogos y Geofísicos del Petróleo, 2009), p. 10.

119. H. Campos, P. Mann, Tectonostratigraphic evolution of the Northern Llanos Foreland Basin of Colombia and implications for its hydrocarbon potential, in *Petroleum Geology and Potential of the Colombian Caribbean Margin*, C. Bartolini, P. Mann, Eds., vol. 108 of *AAPG Memoir* (American Association of Petroleum Geologists, 2015), pp. 517–546.

120. M. Parra, A. Mora, C. Jaramillo, V. Torres, G. Zeilinger, M. R. Strecker, Tectonic controls on Cenozoic foreland basin development in the north-eastern Andes, Colombia. *Basin Res.* **22**, 874–903 (2010).

121. A. Gomez, C. Jaramillo, M. Parra, A. Mora, Huesser horizon: A lake and a marine incursion in Northwestern South America during early Miocene. *Palaios* **24**, 199–210 (2009).

122. M. R. Mello, E. A. M. Koutsoukos, W. U. Mohriak, G. Bacoccoli, Selected petroleum systems in Brazil, in *The Petroleum System: From Source to Tap,* L. B. Magoon, W. G. Dow, Eds., vol. 60 of *AAPG Memoir* (American Association of Petroleum Geologists, 1994), pp. 499–512.

123. M. García-González, L. E. Cruz-Guevara, R. Mier-Umaña, Prospectividad de hidrocarburos en la cuenca Vaupés-Amazonas, Colombia. *Bol. Geol. (Univ. Ind. Santander)* **35**, 15–29 (2013).

124. J. F. Eiras, C. R. Becker, E. M. Souza, J. E. F. Gonzaga, L. M. Silva, L. M. F. Daniel, F. J. Feijó, Bacia do Solimões. *Boletim de Geociências Petrobrás* **8**, 17–45 (1994).

125. R. G. N. Maia, H. K. Godoy, H. S. Yamaguti, P. A. de Moura, F. S. F. da Costa, M. A. de Holanda, J. A. de Costa, *Projeto Carvão no Alto Solimões: Relatório Final* (Serviço Geológico do Brasil–Departamento Nacional de Produção Mineral, 1977).

126. E. A. Lenoir, G. F. Hart, in Burdigalian (early Miocene) Dinocysts from Offshore Louisiana (*American Association of Stratigraphic Palynologists Contribution Series no. 17, American Association of Stratigraphic Palynologists*, 1986), pp. 59–81.

127. K. A. F. Zonneveld, F. Marret, G. J. M. Versteegh, K. Bogus, S. Bonnet, I. Bouimetarhan, E. Crouch, A. de Vernal, Atlas of modern dinoflagellate cyst distribution based on 2405 data points. *Rev. Palaeobot. Palynol.* **191**, 1–197 (2013).

128. B. Dale, in *Palynology: Principles and Applications,* J. Jansonius, D. C. McGregor, Eds. (American Association of Stratigraphic Palynologists Foundation, 1996), pp. 1249–1275.

129. R. A. Fensome, F. J. R. Taylor, G. Norris, W. A. S. Sarjeant, D. I. Wharton, G. L. Williams, *A Classification of Fossil and Living Dinoflagellates,* vol. 7 of *Micropaleontology Special Publication* (Sheridan Press, 1993), 351 pp.

130. J. A. Hopkins, F. M. G. McCarthy, Post-depositional palynomorphs degradation in Quaternary shelf sediments: A laboratory experiment studying the effects of progressive oxidation. *Palynology* **26**, 167–184 (2002).

131. U. Biffi, D. Grignani, Peridinioid dinoflagellate cysts from the Oligocene of the Niger Delta, Nigeria. *Micropaleontology* **29**, 126–145 (1983).

132. S. L. Duffield, J. A. Stein, in Peridiniacean-Dominated Dinoflagellate Cyst Assemblages from the Miocene of the Gulf of Mexico Shelf, Offshore Louisiana (American Association of Stratigraphic Palynologists Contribution Series no. 17, American Association of Stratigraphic Palynologists, 1986), pp. 27–45.

133. C. R. Gilbert, A revision of the hammerhead sharks (family Sphyrnidae). *Proc. U.S. Nat. Mus.* **119**, 1–88 (1967).

134. R. W. Purdy, V. P. Schneider, S. P. Applegate, J. H. McLellan, R. L. Meyer, B. H. Slaughter, The Neogene sharks, rays, and bony fishes from Lee Creek Mine, Aurora, North Carolina. *Smithsonian Contrib. Paleobiol.* **90**, 71–202 (2001).

135. C. T. von Siebold, in *Lehrbuch der vergleichenden Anatomie,* C. T. von Siebold, H. Stannius, Eds. (Verlag von Veit & Company, 1848), pp. 1–679.

136. P. A. Latreille, G. L. L. Buffon, J. E. de Sève, C. S. Sonnini, *Histoire Naturelle, Générale et Particulière des Crustacés et des Insectes: Ouvrage Faisant Suite aux Oeuvres de Leclerc de Buffon, et Partie du Cours Complet d'Histoire Naturelle Rédigé* (F. Dufart, 1802), vol. 3.

137. G. Cuvier, P. A. Latreille, *Le Règne Animal Distribué d'Après son Organisation, Pour Servir de Base à l'Histoire Naturelle des Animaux et d'Introduction à l'Anatomie Comparée* (C. Déterville, 1829).

138. C. Haug, K. R. Shannon, T. Nyborg, F. J. Vega, Isolated mantis shrimp dactyli from the Pliocene of North Carolina and their bearing on the history of Stomatopoda. *Bol. Soc. Geol. Mex.* **65**, 273–284 (2013).

139. S. T. Ahyong, Phylogenetic analysis of the Squilloidea (Crustacea: Stomatopoda). *Invertebr. Syst.* **19**, 189–208 (2005).

140. R. Atkinson, C. Froglia, E. Arneri, B. Antolini, Observations on the burrows and burrowing behaviour of: Squilla mantis L. Crustacea: Stomatopoda. *Mar. Ecol.* **18**, 337–359 (1997).

141. F. Parnaud, Y. Gou, J.-C. Pacual, M. A. Capello, I. Truskowski, H. Passalacqua, in *Petroleum basins of South America,* A. J. Tankard, R. Suárez Soruco, H. J. Welsink, Eds., vol. 62 of *AAPG Memoir* (American Association of Petroleum Geologists, 1995), pp. 681–698.

142. M. A. Bermúdez, B. P. Kohn, P. A. van der Beek, M. Bernet, P. B. O'Sullivan, R. Shagam, Spatial and temporal patterns of exhumation across the Venezuelan Andes: Implications for Cenozoic Caribbean geodynamics. *Tectonics* **29**, 2–21 (2010).

143. F. Parnaud, Y. Gou, J.-C. Pacual, I. Trukowski, O. Gallango, H. J. Welsink, in *Petroleum Basins of South America,* A. J. Tankard, R. Suárez Soruco, H. J. Welsink, Eds., vol. 62 of *AAPG Memoir* (American Association of Petroleum Geologists, 1995), pp. 741–756.

144. A. Mora, W. Casallas, R. Ketcham, D. Gomez, M. Parra, J. Namson, D. F. Stockli, A. A. Vazquez, W. Robles, B. Ghorbal, Kinematic restoration of contractional basement structures using thermokinematic model: A key tool for petroleum system modeling. *AAPG Bull.* **99**, 1575–1598 (2015).

145. B. de Boer, R. S. W. van de Wal, R. Bintanja, L. J. Lourens, E. Tuenter, Cenozoic global ice-volume and temperature simulations with 1-D ice-sheet models forced by benthic $\delta^{18}O$ records. *Ann. Glaciol.* **51**, 23–33 (2010).

146. J. H. Germeraad, C. A. Hopping, J. Muller, Palynology of Tertiary sediments from tropical areas. *Rev. Palaeobot. Palynol.* **6**, 189–348 (1968).

147. C. Jaramillo, M. Rueda, in *III Convención Técnica Asociación Colombiana de Geólogos y Geofísicos del Petroleo (ACGGP) (La inversión en el conocimiento geológico)* (Asociación Colombiana de Geólogos y Geofísicos del Petróleo, 2004), vol. P4 CDROM.

148. C. Jaramillo, M. Rueda, G. Bayona, C. Santos, P. Florez, F. Parra, in *Geological Problem Solving with Microfossils: A Volume in Honor of Garry D. Jones,* T. Demchuk, R. Waszczak, Eds., vol. 93 of *SEPM Special Publication* (SEPM Society For Sedimentary Geology, 2009), pp. 29–40.

149. J. Muller, E. Di Giacomo, A. W. Van Erve, in *A Palynologic Zonation for the Cretaceous, Tertiary and Quaternary of Northern South America* (American Association of Stratigraphic Palynologists Contribution Series No. 19, American Association of Stratigraphic Palynologists, 1987), pp. 7–76.

150. C. Herrera, thesis, Universidad Simón Bolivar (2008).

151. H. Carvajal-Ortiz, G. Mora, C. Jaramillo, A molecular evaluation of a terrestrial correlations: An example from two Paleocene–Eocene of tropical sequences. *Palaeogeogr. Palaeoclimatol. Palaeoecol.* **277**, 173–183 (2009).

152. C. Jaramillo, M. J. Rueda, G. Mora, Cenozoic plant diversity in the neotropics. *Science* **311**, 1893–1896 (2006).

153. C. Jaramillo, D. Ochoa, L. Contreras, M. Pagani, H. Carvajal-Ortiz, L. M. Pratt, S. Krishnan, A. Cardona, M. Romero, L. Quiroz, G. Rodriguez, M. J. Rueda, F. de la Parra, S. Morón, W. Green, G. Bayona, C. Montes, O. Quintero, R. Ramirez, G. Mora, S. Schouten, H. Bermudez, R. Navarrete, F. Parra, M. Alvarán, J. Osorno, J. L. Crowley, V. Valencia, J. Vervoort, Effects of rapid global warming at the Paleocene-Eocene boundary on neotropical vegetation. *Science* **330**, 957–961 (2010).

154. W. H. Blow, in *Proceedings of the First International Conference on Planktonic Microfossils, Geneva, 1967* (E. J. Brill, 1969), vol. 1, pp. 199–421.

155. H. M. Bolli, J.-P. Beckmann, J. B. Saunders, *Benthic foraminiferal Biostratigraphy of the South Caribbean Region* (Cambridge Univ. Press, 1994), pp. 408.

156. L. Díaz de Gamero, in *V Congreso Geologico de Venezuela Memorias,* A. Espejo, Ed. (Sociedad Venezolana de Géologos, 1977), vol. 1, pp. 81–86.

157. M. L. Díaz de Gamero, Estratigrafía y micropaleontología del Oligoceno y Mioceno inferior del centro de la cuenca de Falcón, Venezuela. *GEOS* **22**, 2–54 (1977).

158. M. L. Díaz de Gamero, in *VI Congreso Geologico Venezuela* (Sociedad Venezolana de Géologos, 1985), vol. 1, pp. 454–502.

159. M. L. Díaz de Gamero, El Mioceno temprano y medio de Falcón septentrional. *GEOS* **29**, 25–35 (1989).

160. M. L. Díaz de Gamero, G. Giffuni, M. Castro-Mora, Las formaciones Caujarao y Turupía al este de Cumarebo, Falcón nororiental. *Bol. Soc. Venez. Geol.* **22**, 56–64 (1997).

161. M. L. Díaz de Gamero, O. J. Linares, in *VII Congreso Geologico Venezuela* (Sociedad Venezolana de Géologos, 1989), vol. 1, pp. 419–439.

162. M. L. Díaz de Gamero, V. Mitacchione, M. Ruiz, La Formación Querales en su área tipo, Falcón noroccidental, Venezuela. *Bol. Soc. Venez. Geol.* **34**, 34–46 (1988).

163. O. Linares, Bioestratigrafía de las faunas de mamíferos de las formaciones Socorro, Urumaco y Codore (Mioceno Medio-Plioceno Temprano, de la región de Urumaco, Falcon, Venezuela). *Paleobiología Neotropical* **1**, 1–26 (2004).

164. H. H. Renz, *Stratigraphy and Fauna of the Agua Salada Group, State of Falcon, Venezuela,* vol. 32 of *Geological Society of American Memoirs* (Geological Society of America, 1948), 219 pp.

165. O. Rey, thesis, Universidad Central de Venezuela (1990).

166. J. Wozniak, M. H. Wozniak, Bioestratigrafía de la región nor-central de la Serranía de Falcón, Venezuela nor-occidental. *Bol. Geol.* **16**, 101–139 (1987).

167. K. E. J. Campbell, C. D. Frailey, L. Romero-Pittman, The late Miocene gomphothere *Amahuacatherium peruvium* (Proboscidea: Gomphotheriidae) from the Amazonian Peru: Implications for the great American faunal interchange. *Instituto Geológico Min. Metal.* **23**, 1–151 (2000).

168. K. E. J. Campbell Jr., M. Heizler, C. D. Frailey, L. Romero-Pitman, D. R. Prothero, Upper Cenozoic chronostratigraphy of the southwestern Amazon Basin. *Geology* **29**, 595–598 (2001).

169. G. Bayona, A. Cardona, C. Jaramillo, A. Mora, C. Montes, V. Caballero, H. Mahecha, F. Lamus, O. Montenegro, G. Jimenez, A. Mesa, V. Valencia, in *Thick-Skin-Dominated Orogens: From Initial Inversion to Full Accretion,* M. Nemcok, A. R. Mora, J. W. Cosgrove, Eds., vol. 377 of *Geological Society of London Special Publication* (Geological Society of London, 2013), pp. 285–314.

170. G. Rodríguez-Forero, F. E. Oboh-Ikuenobe, C. Jaramillo-Munoz, M. Rueda-Serrano, E. Cadena-Rueda, Palynology of the Eocene Esmeraldas Formation, Middle Magdalena Valley Basin, Colombia. *Palynology* **36**, 96–111 (2012).

171. B. I. Kronberg, R. E. Benchimol, M. I. Bird, Geochemistry of Acre subbasin sediments: Window on ice-age Amazonia. *Interciencia* **16**, 138–141 (1991).

172. D. Santos, L. Silva, O Exogeossinclíneo Andino e a Formação Solimões, in *Anais do 29° Congresso Brasileiro de Geologia* (Sociedade Brasileira de Geologia, 1976), pp. 135–147.

173. D. de Fátima Rossetti, P. M. de Toledo, A. M. Góes, New geological framework for Western Amazonia (Brazil) and implications for biogeography and evolution. *Quat. Res.* **63**, 78–89 (2005).

174. H. Tuomisto, K. Ruokolainen, J. Salo, Lago Amazonas: Fact or fancy. *Acta Amazon.* **22**, 353–361 (1992).

175. K. Matsuoka, Late Cenozoic dinoflagellates and acritarchs in the Niigata District, central Japan. *Paleontographica B* **187**, 89–154 (1983).

176. G. L. Eaton, R. A. Fensome, J. B. Riding, G. L. Williams, Re-evaluation of the status of the dinoflagellate cyst genus Cleistosphaeridium. *Neues. Jahrb. Geol. Paläontol. Abh.* **219**, 171–205 (2001).

177. M. Schreck, J. Matthiessen, M. J. Head, A magnetostratigraphic calibration of middle Miocene through Pliocene dinoflagellate cyst and acritarch events in the Iceland Sea (Ocean Drilling Program Hole 907A). *Rev. Palaeobot. Palynol.* **187**, 66–94 (2012).

178. A. Soliman, S. Ćorić, M. J. Head, W. E. Piller, S. Y. El Beialy, Lower and middle Miocene biostratigraphy, Gulf of Suez, Egypt based on dinoflagellate cysts and calcareous nannofossils. *Palynology* **36**, 38–79 (2012).

179. L. de Verteuil, in *Proceedings of the Ocean Drilling Program: Scientific Results,* G. S. Mountain, K. G. Miller, P. Blum, C. W. Poag, D. C. Twichell, Eds. (Ocean Drilling Program, 1996), vol. 150, pp. 439–454.

180. L. de Verteuil, G. Norris, Miocene dinoflagellate stratigraphy and systematics of Maryland and Virginia. *Micropaleontology* **42**, 1–172 (1996).

181. K. Matsuoka, M. J. Head, in *Neogene and Quaternary Dinoflagellate Cysts and Acritarchs,* M. J. Head, J. H. Wrenn, Eds. (American Association of Stratigraphic Palynologists Foundation, 1992), pp. 165–180.

182. J. Zachos, M. Pagani, L. Sloan, E. Thomas, K. Billups, Trends, rhythms, and aberrations in global climate 65 Ma to present. *Science* **292**, 686–693 (2001).

183. P.-O. Antoine, M. A. Abello, S. Adnet, A. J. A. Sierra, P. Baby, G. Billet, M. Boivin, Y. Calderón, A. Candela, J. Chabain, F. Corfu, D. A. Croft, M. Ganerød, C. Jaramillo, S. Klaus, L. Marivaux, R. E. Navarrete, M. J. Orliac, F. Parra, M. E. Pérez, F. Pujos, J.-C. Rage, A. Ravel, C. Robinet, M. Roddaz, J. V. Tejada-Lara, J. Vélez-Juarbe, F. P. Wesselingh,

R. Salas-Gismondi, A 60-million-year Cenozoic history of western Amazonian ecosystems in Contamana, eastern Peru. *Gondw. Res.* **31**, 30–59 (2015).

184. C. Amante, B. W. Eakins, ETOPO1 1 Arc-Minute Global Relief Model: Procedures, Data Sources and Analysis (Technical Memorandum NESDIS NGDC-24, National Oceanic and Atmospheric Administration, 2009).

185. U.S. Geological Survey, *Global 30 Arc-Second Elevation (GTOPO30)* (U.S. Geological Survey, 2015); https://lta.cr.usgs.gov/GTOPO30.

Citation: C. Jaramillo, I. Romero, C. D'Apolito, G. Bayona, E. Duarte, S. Louwye, J. Escobar, J. Luque, J. D. Carrillo-Briceño, V. Zapata, A. Mora, S. Schouten, M. Zavada, G. Harrington, J. Ortiz, F. P. Wesselingh, Miocene flooding events of western Amazonia. *Sci. Adv.* **3**, e1601693 (2017).

The following resources related to this article are available online at
http://advances.sciencemag.org. (This information is current as of May 3, 2017):

Updated information and services, including high-resolution figures, can be found in the
online version of this article at:
http://advances.sciencemag.org/content/3/5/e1601693.full

Supporting Online Material can be found at:
http://advances.sciencemag.org/content/suppl/2017/05/01/3.5.e1601693.DC1

This article **cites 126 articles,** 32 of which you can access for free at:
http://advances.sciencemag.org/content/3/5/e1601693#BIBL